Extended-Range Spectroscopic pH Measurement Using Optimized Mixtures of Dyes

B. RAGHURAMAN,* G. GUSTAVSON, R. E. G. VAN HAL, E. DRESSAIRE,† and O. ZHDANEEV
Schlumberger-Doll Research, Ridgefield, Connecticut 06877

The spectroscopic technique for pH measurement is a well-established laboratory technique that can give high-accuracy pH values. Recent studies have shown the advantage of this technique over standard potentiometric methods for pH measurements in fresh water and seawater and also at high temperatures and pressures. However, a limitation of the spectroscopic technique is that a single pH dye is sensitive only over a narrow pH range. We have developed optimized dye mixtures that are both sensitive and accurate over a broad pH range. The measurement is robust and simple, requires a minimum of two wavelengths, and is independent of the volume of the dye mixture added. Optimization of the dye mixture formulation to maximize accuracy in a broad range of pH involves varying both the dye type and its mole fraction and also accounting for spectral noise. This technique has been successfully applied for *in situ* pH measurements of oilfield formation waters.

Index Headings: **Spectroscopic pH; Extended-range pH; pH dye mixtures.**

INTRODUCTION

Potentiometric techniques that are commonly used for pH measurements are recommended only for temperatures in the range 278–323 °K, pressure of 0.1 Mpa, and ionic strengths below 0.1 mol/kg water.[1] The reason for this measurement constraint is the uncertainty in liquid junction potential and reference electrode stability at high temperatures, high pressures, and very low and high ionic strength. The spectroscopic (or colorimetric) method for pH measurement is a well-established technique that employs a pH-sensitive dye that changes color depending on the pH of the solution.[2–6] Recent publications show the advantage of the spectroscopic technique over the electrode technique with respect to low drift, reproducibility, and rapidness of the measurement for seawater (high ionic strength) and freshwater (low ionic strength).[4–6] The spectroscopic technique has also been applied successfully to high temperature and pressure measurements of oilfield brines in oil wells.[7,8]

The principle of the spectroscopic measurement is that the pH-sensitive dyes can exist in an acid or base form. The optical absorbance spectra of pH-sensitive dyes change as they convert from their acid (A) to base form (B) (see Fig. 1):

$$A \Leftrightarrow B + H^+ \tag{1}$$

The fraction of the dye present in the acid and base forms depends on the pH of the solution. The pH is calculated using Eq. 2:

$$\mathrm{pH} = \mathrm{p}K_a + \log\frac{\gamma_B}{\gamma_A} + \log\frac{[B]}{[A]} \tag{2}$$

where $\mathrm{p}K_a = -\log K_a$, K_a is the thermodynamic equilibrium constant for the dye dissociation (Eq. 1) and is a function of temperature and pressure, [A] and [B] are the concentrations of the acid and base form of the dye in the dye–sample mixture, respectively, and γ_A and γ_B are the activity coefficients of the acid and base forms of the dye and are a function of the temperature, pressure, and ionic strength of the solution.

Equation 2 is more commonly written as:

$$\mathrm{pH} = \mathrm{p}K'_a + \log\frac{[B]}{[A]} \tag{3}$$

where

$$\mathrm{p}K'_a = -\log\left(K_a\frac{\gamma_A}{\gamma_B}\right) \tag{4}$$

Because $\mathrm{p}K'_a$ includes the activity coefficients, it is no longer a function only of pressure and temperature, but also a function of ionic strength.

The ratio of the indicator that exists in the base form to the acid form ([B]/[A]) may be calculated from spectral measurements as shown below:

$$C_T = [A] + [B] \tag{5}$$

$$OD^{\lambda 1} = \varepsilon_A^{\lambda 1} l[A] + \varepsilon_B^{\lambda 1} l[B] \tag{6}$$

$$OD^{\lambda 2} = \varepsilon_A^{\lambda 2} l[A] + \varepsilon_B^{\lambda 2} l[B] \tag{7}$$

$$ODR_{\lambda 1}^{\lambda 2} = \frac{OD^{\lambda 2}}{OD^{\lambda 1}} \tag{8}$$

$$\frac{[B]}{[A]} = \frac{ODR_{\lambda 1}^{\lambda 2}}{\frac{\varepsilon_B^{\lambda 2}}{\varepsilon_A^{\lambda 1}}} \frac{\left(1 - \frac{\varepsilon_A^{\lambda 2}}{\varepsilon_A^{\lambda 1}}\frac{1}{ODR_{\lambda 1}^{\lambda 2}}\right)}{\left(1 - \frac{\varepsilon_B^{\lambda 1}}{\varepsilon_B^{\lambda 2}} ODR_{\lambda 1}^{\lambda 2}\right)} \tag{9}$$

where $OD^{\lambda i}$ is the optical density measured at wavelength λ_i, l is the path length in cm, [A] and [B] are the concentrations of the acid and base forms in the sample–dye mixture in mol/kg, C_T is the total dye concentration in the sample–dye mixture in mol/kg, $\varepsilon_A^{\lambda i}$ and $\varepsilon_B^{\lambda i}$ are the molar extinction coefficients at wavelength λ_i for A and B in $(\mathrm{mol/kg})^{-1}\mathrm{cm}^{-1}$, and $ODR_{\lambda 1}^{\lambda 2}$ is the optical density ratio as defined in Eq. 8.

Calibration of the dye for pH measurement of unknown water samples requires determination of $\mathrm{p}K'_a$ and the molar extinction coefficients of the acid and base forms. This is usually done by spectroscopic measurements of dye in buffer solutions at the two extreme pH values (end points) where the dye exists only in the acid or base form, and also in the intermediate pH range where both forms exist (see Fig. 1). Equation 9 can be used to calculate the base-to-acid

Received 13 June 2006; accepted 8 September 2006.
* Author to whom correspondence should be sent. E-mail: bhavani@slb.com.
† Present address: DEAS, Harvard University, Cambridge, MA, USA.

0003-7028/06/6012-1461$2.00/0

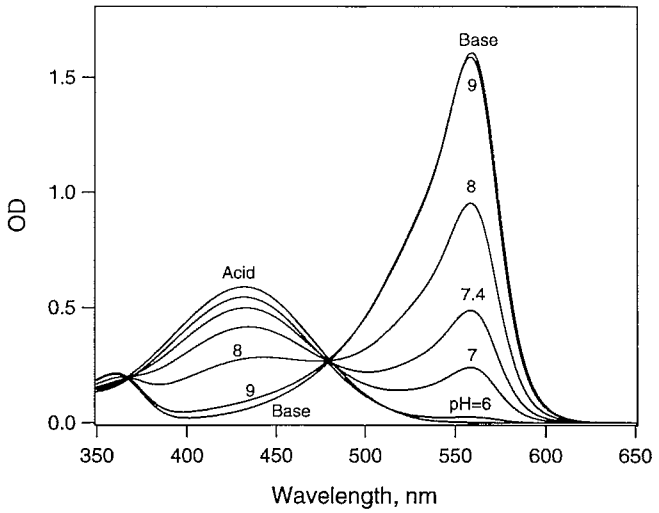

FIG. 1. Phenol red spectra in various buffer solutions at 293 °K. The acid form spectrum was obtained in a pH 4 buffer and the base form spectrum in pH 10 buffer. The dye concentration is 3.18×10^{-5} mol/kg. Spectral path length is 1 cm.

concentration ratios for the dye spectra in the standard pH buffer solutions. Using Eq. 3, pK_a' can be obtained from the intercept of the plot of pH versus log([B]/[A]). Once pK_a' is known from this calibration, the pH of any unknown solution can be obtained spectroscopically using Eqs. 3 and 9. Note that since the acid and base form concentrations appear only as a ratio in Eq. 3 and the absolute concentration of the dye does not appear in Eq. 9, the pH calculation is independent of the dye concentration in the sample. The only requirements for the dye addition are that the concentration be (1) within a range where Beer's law is satisfied, (2) below an upper limit depending on the buffer strength of the sample, beyond which the addition of the dye could alter the sample pH, and (3) above a lower limit where the OD values are such that the signal-to-noise ratio is acceptable.

In principle, one can also obtain the pH by measuring absorption at a single wavelength if the total dye concentration is known very accurately. However, this method is not quite as robust as using the concentration-independent two-wavelength approach as even small errors in the absolute concentration (C_T) can cause large errors in the pH calculation. One can also calculate the pH by using the full spectral scan in the visible region and applying regression analysis to obtain the base-to-acid ratio.

The main limitation of the spectroscopic technique is the limited range of pH sensitivity of each dye, typically 2–3 units. Figure 1 shows the optical spectra of a dye (pK_a' equal to 7.79) in several standard buffer solutions of varying pH values. For pH values below 6, the dye exists mostly in its acid form with a single peak at 432 nm. For pH values above 9, the dye is mostly in its base form with a peak at 559 nm. At all pH values between 6 and 9, both forms exist. As one increases the pH from 6 to 9, the OD drops at the acid-peak wavelength and increases at the base-peak wavelength. The dye is most sensitive to the pH of the sample when the acid and base absorptions are equal, and the sensitivity drops as the pH moves away from the pK_a' value in either direction. As seen from Eq. 3, for example, when the pH and pK_a' are more than two units apart, the base or acid fractions become less than 1% of the total dye added and the corresponding OD value becomes too small to be measured accurately. To measure pH outside this range, one must choose a different dye with a different pK_a' value. Thus, the approximate pH range of the sample must be deduced or known *a priori* so that the correct dye can be chosen for the measurement.

Using a mixture of dyes as is done for the commonly used universal indicator solution can extend the range of pH measurement. Estimation of pH is done visually by color comparison and hence accuracy is low (on the order of 0.5 to 1 pH units).[2] Higher accuracy through spectroscopy is difficult because the visible spectrum of a mixture of dyes is a cumulative addition of the spectra of the individual dyes. Unless the individual spectra are well resolved, it is difficult to invert the acid and base fractions of the dye for an accurate pH calculation. Selection of dyes and optimization of their concentrations to extend the measurement range have been described in the literature,[9–11] but each of these approaches have their limitations, which we discuss in more detail in the Results and Discussion section.

In this paper, a methodology is proposed for formulating dye mixtures that allows extended-range and high-accuracy spectroscopic pH measurements. The key features of the approach proposed here include an efficient formulation of the objective function and the consideration of the spectral measurement noise in the optimization process. This gives the optimum dye formulation together with the expected precision in the measurement at each pH over the target interval. We first describe the theory and the optimization algorithms for formulating these dye mixtures and then show its application with laboratory measurements. Application to measurement of pH of oilfield brines using dye mixtures in an oil well is also presented. Downhole measurements on water samples in their native conditions are more robust than bringing samples up-hole to surface laboratories because the change in temperature and pressure could potentially cause dissolved gases or solids to come out of solution and alter the pH. Potentiometric methods are difficult to implement at these downhole conditions of high temperature and pressures and there is also the potential of fouling of the electrode surfaces from oils and drilling muds. Spectroscopic pH measurement is hence attractive. Real-time measurement downhole in oil wells requires carrying the dye solution on a tool where space and weight constraints exist. By using an optimized dye mixture solution, a single reservoir for the dye is sufficient on the tool and can target the typical range of oilfield water pH values (typically 3 to 9 units).

EXPERIMENTAL

All laboratory spectra were measured with a Cary 500 UV-Visible-NIR spectrometer at 293 °K. NIST certified standard buffer solutions were obtained from Fisher Scientific. Sodium salts of phenol red, chlorophenol red, and bromophenol blue (Fisher Scientific) were purchased as solid powder and solutions of desired strengths were prepared.

THEORY

We derive below the pH calculation model for a two-dye mixture and extend it to three and more dyes.

Modeling Dye Mixtures. Equations 2–8 may be rewritten for two dyes as follows:

$$\mathrm{pH} = \mathrm{p}K_{a1} + \log\frac{\gamma_{B1}}{\gamma_{A1}} + \log\frac{[B_1]}{[A_1]} \tag{10}$$

$$\mathrm{pH} = \mathrm{p}K_{a2} + \log\frac{\gamma_{B2}}{\gamma_{A2}} + \log\frac{[B_2]}{[A_2]} \tag{11}$$

$$C_{T1} = [A_1] + [B_1] \tag{12}$$

$$C_{T2} = [A_2] + [B_2] \tag{13}$$

$$f_1 = \frac{C_{T1}}{C_{T1} + C_{T2}} \tag{14}$$

$$\mathrm{OD}^{\lambda 1} = \varepsilon_{A1}^{\lambda 1} l[A_1] + \varepsilon_{B1}^{\lambda 1} l[B_1] + \varepsilon_{A2}^{\lambda 1} l[A_2] + \varepsilon_{B2}^{\lambda 1} l[B_2] \tag{15}$$

$$\mathrm{OD}^{\lambda 2} = \varepsilon_{A1}^{\lambda 2} l[A_1] + \varepsilon_{B1}^{\lambda 2} l[B_1] + \varepsilon_{A2}^{\lambda 2} l[A_2] + \varepsilon_{B2}^{\lambda 2} l[B_2] \tag{16}$$

$$\mathrm{ODR}_{\lambda 1}^{\lambda 2} = \frac{\mathrm{OD}^{\lambda 2}}{\mathrm{OD}^{\lambda 1}} \tag{17}$$

where $[A_1]$ and $[B_1]$ are the acid and base form concentrations of dye 1 in the sample–dye mixture, $[A_2]$ and $[B_2]$ are the acid and base form concentrations of dye 2 in the sample–dye mixture, C_{T1} and C_{T2} are the total concentrations of dye 1 and dye 2 in the sample–dye mixture, f_1 is the mole fraction of dye 1 in the dye mixture, and $\mathrm{p}K_{a1}$ and $\mathrm{p}K_{a2}$ are the dissociation constants for dyes 1 and 2.

From Eqs. 10–17, one can write:

$$\mathrm{ODR}_{\lambda 1}^{\lambda 2} = \frac{\sum_i \frac{[B_i]}{[B_1]} \varepsilon_{Bi}^{\lambda 2}\left[1 + \frac{\varepsilon_{Ai}^{\lambda 2}}{\varepsilon_{Bi}^{\lambda 2}} 10^{-(\mathrm{pH}-\mathrm{p}K'_{ai})}\right]}{\sum_i \frac{[B_i]}{[B_1]} \varepsilon_{Ai}^{\lambda 1}\left[10^{-(\mathrm{pH}-\mathrm{p}K'_{ai})} + \frac{\varepsilon_{Bi}^{\lambda 1}}{\varepsilon_{Ai}^{\lambda 1}}\right]} \quad \text{for } i = 1,2 \tag{18}$$

where

$$\frac{[B_2]}{[B_1]} = \frac{1 + 10^{-(\mathrm{pH}-\mathrm{p}K'_{a1})}}{1 + 10^{-(\mathrm{pH}-\mathrm{p}K'_{a2})}} \frac{(1 - f_1)}{f_1} \tag{19}$$

Hence,

$$\mathrm{ODR}_{\lambda 1}^{\lambda 2} = F(\mathrm{pH}, \varepsilon, \mathrm{p}K'_{a1}, \mathrm{p}K'_{a2}, f_1) \tag{20}$$

where

$$\varepsilon = (\varepsilon_{A1}^{\lambda 1}, \varepsilon_{B1}^{\lambda 1}, \varepsilon_{A1}^{\lambda 2}, \varepsilon_{B1}^{\lambda 2}, \varepsilon_{A2}^{\lambda 1}, \varepsilon_{B2}^{\lambda 1}, \varepsilon_{A2}^{\lambda 2}, \varepsilon_{B2}^{\lambda 2}) \tag{21}$$

Thus, from Eq. 20, we see that once the two-dye mixture is chosen and the wavelengths are selected, the optical density ratio, $\mathrm{ODR}_{\lambda 1}^{\lambda 2}$, is a function only of the pH. It is independent of the total dye concentration in the sample, and therefore retains the advantages of the single-dye measurement. One could invert function F to express pH as a function of $\mathrm{ODR}_{\lambda 1}^{\lambda 2}$, but the analytical expression is very long and complex. In practice it is simpler to generate either a plot or a look-up table for $\mathrm{ODR}_{\lambda 1}^{\lambda 2}$ as a function of pH for a given dye mixture and a set of wavelengths using Eq. 18. This procedure then gives pH as a discrete function of $\mathrm{ODR}_{\lambda 1}^{\lambda 2}$.

Equations 10 through 21 can be easily extended to a system of n dyes to give:

$$\mathrm{ODR}_{\lambda 1}^{\lambda 2} = \frac{\sum_i \frac{[B_i]}{[B_1]} \varepsilon_{Bi}^{\lambda 2}\left[1 + \frac{\varepsilon_{Ai}^{\lambda 2}}{\varepsilon_{Bi}^{\lambda 2}} 10^{-(\mathrm{pH}-\mathrm{p}K'_{ai})}\right]}{\sum_i \frac{[B_i]}{[B_1]} \varepsilon_{Ai}^{\lambda 1}\left[10^{-(\mathrm{pH}-\mathrm{p}K'_{ai})} + \frac{\varepsilon_{Bi}^{\lambda 1}}{\varepsilon_{Ai}^{\lambda 1}}\right]} \quad \text{for } i = 1,n \tag{22}$$

$$\frac{[B_i]}{[B_1]} = \frac{1 + 10^{-(\mathrm{pH}-\mathrm{p}K'_{a1})}}{1 + 10^{-(\mathrm{pH}-\mathrm{p}K'_{ai})}} \frac{f_i}{f_1} \quad \text{for } i = 1,n \tag{23}$$

$$\mathrm{ODR}_{\lambda 1}^{\lambda 2} = F(\mathrm{pH}, \varepsilon, \mathrm{p}K'_{a1}, \mathrm{p}K'_{a2}, \ldots, \mathrm{p}K'_{an}, f_1, f_2, \ldots, f_n) \tag{24}$$

where

$$\varepsilon = (\varepsilon_{A1}^{\lambda 1}, \varepsilon_{B1}^{\lambda 1}, \varepsilon_{A1}^{\lambda 2}, \varepsilon_{B1}^{\lambda 2}, \varepsilon_{A2}^{\lambda 1}, \varepsilon_{B2}^{\lambda 1}, \varepsilon_{A2}^{\lambda 2}, \varepsilon_{B2}^{\lambda 2}, \ldots, \varepsilon_{An}^{\lambda 1}, \varepsilon_{Bn}^{\lambda 1}, \varepsilon_{An}^{\lambda 2}, \varepsilon_{Bn}^{\lambda 2}) \tag{25}$$

Hence,

$$\mathrm{pH} = F^{-1}(\mathrm{ODR}_{\lambda 1}^{\lambda 2}, \varepsilon, \mathrm{p}K'_{a1}, \mathrm{p}K'_{a2}, \ldots, \mathrm{p}K'_{an}, f_1, f_2, \ldots, f_n) \tag{26}$$

One can generate a plot or table of $\mathrm{ODR}_{\lambda 1}^{\lambda 2}$ as a function of pH and hence determine the pH from the measured $\mathrm{ODR}_{\lambda 1}^{\lambda 2}$.

The pH as calculated from Eq. 26, however, is not necessarily always a unique function of $\mathrm{ODR}_{\lambda 1}^{\lambda 2}$. Figure 2a shows a plot where two dyes ($\mathrm{p}K'_{a1} = 7.79$, $\mathrm{p}K'_{a2} = 6.11$, $f_1 = 0.5$) are mirror images of each other where the spectrum of the acid form of one dye is identical to the spectrum of the base form of the second dye and vice versa ($\varepsilon_{A1}^{\lambda j} = \varepsilon_{B2}^{\lambda j}$; $\varepsilon_{A2}^{\lambda j} = \varepsilon_{B1}^{\lambda j}$ for all j). Thus, while for each pH value one obtains a unique $\mathrm{ODR}_{\lambda 1}^{\lambda 2}$, the inverse is not true. That is, for a given $\mathrm{ODR}_{\lambda 1}^{\lambda 2}$, two pH values are possible and the method fails. By choosing dyes that show similar direction of color change (but at different $\mathrm{p}K'_{ai}$ values) with pH, one can increase the sensitivity of the pH to $\mathrm{ODR}_{\lambda 1}^{\lambda 2}$ and obtain a unique solution. Figure 2b shows the pH versus $\mathrm{ODR}_{\lambda 1}^{\lambda 2}$ plot for two dyes ($\mathrm{p}K'_{a1} = 7.79$, $\mathrm{p}K'_{a2} = 6.11$, $f_1 = 0.5$) with identical spectra for acid and base forms ($\varepsilon_{A1}^{\lambda j} = \varepsilon_{A2}^{\lambda j}$; $\varepsilon_{B1}^{\lambda j} = \varepsilon_{B2}^{\lambda j}$ for all j); with these two dyes the method would work well. These results are contrary to the intuitive selection of two dyes for a mixture, where one would expect good spectral resolution to be more beneficial in inverting for acid and base fractions of each dye to calculate pH.

These results highlight that it is important to carefully formulate dye mixtures to make extended-range pH measurements. The sulfonephthalein family of indicators is a good example of a set of indicators with different $\mathrm{p}K'_{ai}$ values that satisfy the requirements of similar direction of color changes. They are also commonly used in spectroscopic pH measurements. We next discuss how we can optimally formulate dye mixtures to maximize precision of the measurement for extended pH ranges.

Formulating Optimized Dye Mixtures. Optimizing dye mixtures could imply minimizing the pH measurement error for a target pH range, or it could imply maximizing the pH range with an acceptable pH measurement error. While the uncertainties in estimation of $\mathrm{p}K'_{ai}$ and molar extinction coefficients propagate as fixed errors into the pH measurement, the dynamic pH measurement error is from the spectroscopic noise in the spectral signal. For a given set of dyes in the

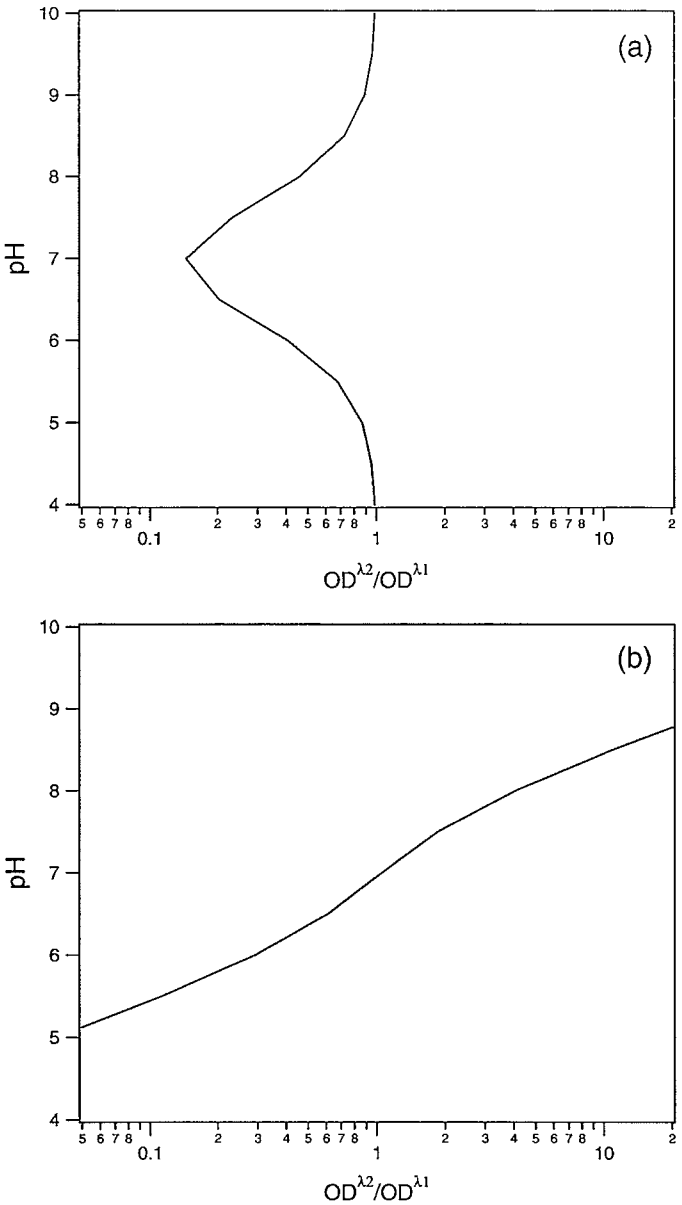

FIG. 2. Mixture of two dyes with different pK'_{ai} values. (**a**) The acid form spectrum of one dye is identical to the base form spectrum of the other and vice versa. This results in the pH being a non-unique function of $ODR^{\lambda 2}_{\lambda 1}$(=$OD^{\lambda 2}/OD^{\lambda 1}$). (**b**) The acid and base forms of the two dyes have identical spectra. The pH is a unique function of $ODR^{\lambda 2}_{\lambda 1}$.

formulation (fixed pK'_{ai}), the control variables are the mole fractions of the individual dyes. Equation 27 is a possible formulation for the objective function to be minimized for a desired standard deviation of 0.01 pH units or less over the interval pH_1 to pH_2:

$$G(f_1, f_2, \ldots, f_n) = \sum_{i=1}^{m} w_i(\sigma_{pH_i} - 0.01)^p \quad \text{for all } \sigma_{pH_i} \geq 0.01 \tag{27}$$

where σ_{pH_i} is the standard deviation in pH at pH_i, m is the number of discreet points into which the interval between pH_1 and pH_2 is divided (pH is a discrete function of $ODR^{\lambda 2}_{\lambda 1}$), w_i is the weight applied to the error contribution at each point, and p is the power factor for the error contribution.

Both w_i and p may be chosen to adjust the contribution of the standard deviation at each pH value in the desired range. This adjustment gives the flexibility of having different levels of precision within a broader constraint of, for example, 0.01 pH units over the entire interval.

To determine the standard deviation in pH measurement as a function of spectroscopic noise (standard deviation in OD), we use the method of error propagation.[12] For a dependent variable x shown in Eq. 28:

$$x = f(u, v) \tag{28}$$

the standard deviation in $x(\sigma_x)$ as a function of standard deviations in $u(\sigma_u)$ and $v(\sigma_v)$ is given as

$$\sigma_x \cong \sqrt{\sigma_u^2 \cdot \left(\frac{\partial x}{\partial u}\right) + \sigma_v^2 \cdot \left(\frac{\partial x}{\partial v}\right)^2} \tag{29}$$

For a given dye mixture (fixed pK'_{ai}, ε, f_i) and for a given set of wavelengths (λ_1, λ_2), one can apply the error propagation algorithm to Eq. 22 and Eq. 26:

$$\sigma_{ODR^{\lambda 2}_{\lambda 1}} = ODR^{\lambda 2}_{\lambda 1} \cdot \sqrt{\left(\frac{\sigma_{OD^{\lambda 2}}}{OD^{\lambda 2}}\right)^2 + \left(\frac{\sigma_{OD^{\lambda 1}}}{OD^{\lambda 1}}\right)^2} \tag{30}$$

$$\sigma_{pH} = \frac{\partial pH}{\partial ODR^{\lambda 2}_{\lambda 1}} \cdot \sigma_{ODR^{\lambda 2}_{\lambda 1}} \tag{31}$$

Combining Eq. 30 and Eq. 31, we get standard deviation in pH measurement (σ_{pH}) as a function of spectroscopic noise at the two wavelengths, λ_1 and λ_2:

$$\sigma_{pH} = \frac{\partial pH}{\partial ODR^{\lambda 2}_{\lambda 1}} \cdot ODR^{\lambda 2}_{\lambda 1} \cdot \sqrt{\left(\frac{\sigma_{OD^{\lambda 2}}}{OD^{\lambda 2}}\right)^2 + \left(\frac{\sigma_{OD^{\lambda 1}}}{OD^{\lambda 1}}\right)^2} \tag{32}$$

The derivative of pH with respect to $ODR^{\lambda 2}_{\lambda 1}$ can be obtained numerically from Eq. 24.

For equal noise at the two wavelengths ($\sigma_{OD^{\lambda 1}} = \sigma_{OD^{\lambda 2}} = \sigma_{OD}$), from Eq. 32, we see that σ_{pH} increases linearly with σ_{OD}. Note also that while the pH calculation is independent of total dye concentration in sample, the standard deviation in the pH measurement depends on the total dye concentration through the absolute optical density values ($OD^{\lambda 1}$, $OD^{\lambda 2}$) that appear in Eq. 32. For a given dye mixture with a fixed mole fraction of the individual dyes, the standard deviation in pH, σ_{pH}, decreases linearly with increasing total dye concentration. However, as explained in the Introduction section, if the concentration of the dye added is very high then it could affect the pH of the sample and introduce additional systematic errors in the measurement.

RESULTS AND DISCUSSION

Table I summarizes the spectral properties of the dyes used in the experiments and simulations. A non-gradient simplex minimization algorithm[13] was used with Eq. 27 to optimize dye mixture formulations. Figure 3 compares the standard deviation in pH for a single dye (phenol red) and for an optimized three-dye mixture containing phenol red, chlorophenol red, and bromophenol blue. These figures can be used in various ways to set specifications for the measurement. For a given target precision of the pH measurement, the pH range for which the single dye and the three-dye mixture would work can be specified. For example, if a standard deviation of 0.01 units is

TABLE I. Summary of dye properties at 293 °K used in simulations.

	Phenol red (PR) (dye 1)		Chlorophenol red (CPR) (dye 2)		Bromophenol blue (BB) (dye 3)	
	Acid	Base	Acid	Base	Acid	Base
ε at 570 nm (λ_2) (mol/kg)$^{-1}$cm^{-1}	108	37975	58	54247	378	46859
ε at 445 nm (λ_1) (mol/kg)$^{-1}$cm^{-1}	17916	3352	18136	1985	21711	1981
Molecular weight	354.38	376.36	423.28	445.26	669.98	691.97
pK'_a at 0.1 mol/kg ionic strength	7.79		6.11		4.11	

acceptable, the three-dye mixture can be used over a pH range from 3.48 to 8.01 pH units, while the phenol red alone would work over a range from 6.58 to 8.64 pH units. Thus, the three-dye mixture allows measurement over a wider range than the individual dye does. Alternately, one could select a pH range and specify the standard deviations at each pH. For example, for the three-dye mixture, at pH 3, the standard deviation would be 0.024 units.

Figure 4 shows the effect of changing the power p in the objective function (Eq. 27). By the nature of the measurement, the error bar is higher at the extremes of the pH range than it is in the middle, even under the optimized conditions. Hence, it is important to ensure the standard deviation contributions at the extremes are not given a disproportionately higher weighting than the standard deviation contributions in the middle of the range. This fact is illustrated in Fig. 4 where at pH equal to 9, the deviation from 0.01 pH units is very high compared to the deviation at a pH equal to 5. By using a power of 1, the contribution of error at pH 9 to the objective function is 0.027 pH units and is about nine times higher than the contribution at pH 5 (0.003 pH units) at the optimum point. However, if the power p is set equal to 0.2, the contribution of the standard deviation at pH 9 (0.48 pH units) to the objective function is only 1.55 times higher than the contribution of the standard deviation at pH 5 (0.31 pH units) and a different optimum point is obtained. In the second case with power p equal to 0.2, the optimization algorithm gives nearly equal importance to minimizing the error at pH 5 and pH 9, while in the first case the pH 9 term dominates and the optimizer ignores the error at pH 5. This is evident in the plots in Fig. 4 where the standard deviation is reduced to below 0.01 units at pH 5 by lowering p and is more uniform across the range of pH.

Figure 5 shows the results for a three-dye mixture optimized for the pH range of 3 to 9 and compares them with the cases where equal-weight and equal-mole fractions are used. The benefit of the optimization is clearly seen with the much broader pH measurement range satisfying the precision requirement for the optimized case as compared to the equal-mole fraction case. The improvement over the equal-weight fraction case is more subtle, with an increase of 0.35 pH units in the pH measurement range for the same standard deviation constraint. Figure 6 shows how the optimizer adjusts mole fractions of the dyes in the mixture as the pH range of interest changes. As one shifts from a pH range of 3 to 9 units to a smaller interval of 6 to 9 units, the fraction of the dye 1 (pK'_{a1} = 7.79) increases while that of dye 3 (pK'_{a3} = 4.11) falls to 0. It is also possible to optimize the dye selection process. Thus, for a fixed mole fraction, one can optimize for pK'_{ai} values of the dyes in the mixture to obtain maximum accuracy in the pH interval of interest. Figure 7 lists optimum sets of pK'_{ai} values of dyes in a three-dye mixture for different pH intervals of interest. For this simulation, the three dyes were at equal weight fractions and epsilon values were fixed as given in Table I. Note how the optimum set of pK'_{ai} values changes depending on the target pH interval. Figure 8 demonstrates the effect of noise in the spectral measurement, σ_{OD}, on the optimization process. For a noise level of 0.001 OD units, the three-dye mixture covers a broad pH target range (3.04–8.71 pH units) with an acceptable standard deviation of 0.01 units. If the noise level is higher at 0.0015 units, but the dye mole

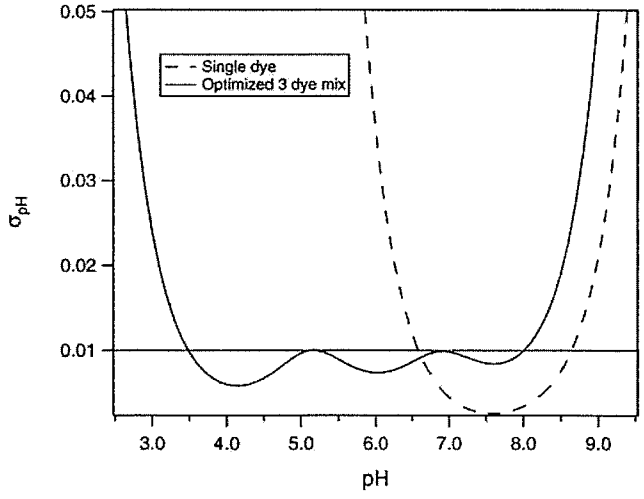

FIG. 3. Standard deviation in pH measurement as a function of pH for single (phenol red dye) and optimized three-dye mixtures. Spectroscopic noise is assumed to be 0.001 OD units. Total dye concentration is 2×10^{-5} mol/kg and $p = 0.2$ in Eq. 27. Optimization interval for pH is 3 to 9 pH units.

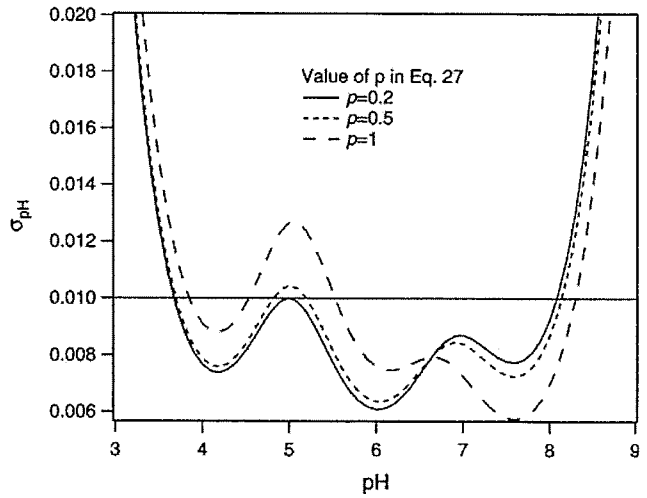

FIG. 4. Effect of changing the power p in the objective function Eq. 27. Total dye concentration is 2×10^{-5} mol/kg and spectral noise is 0.001 OD units. Optimization interval for pH is 4 to 9 pH units.

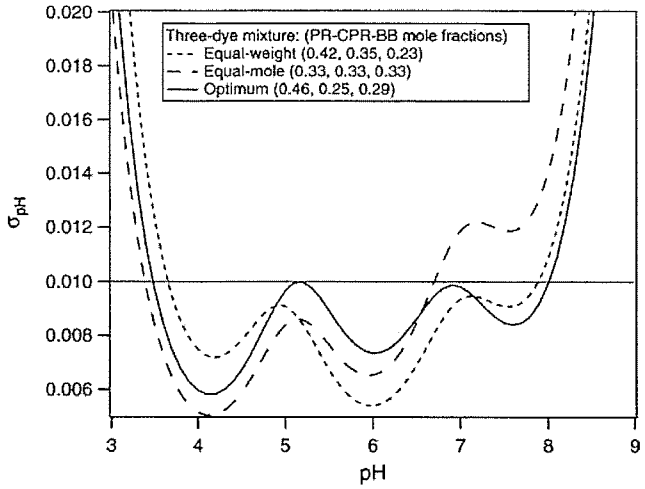

FIG. 5. Standard deviations in pH for optimized three-dye mixtures compared with those for equal-mole and equal-weight fraction mixtures. Spectroscopic noise is assumed to be 0.001 OD units. Total dye concentration is 2×10^{-5} mol/kg (Eq. 27: $p = 0.2$; $w_i = 1$). Optimization interval for pH is 3 to 9 pH units.

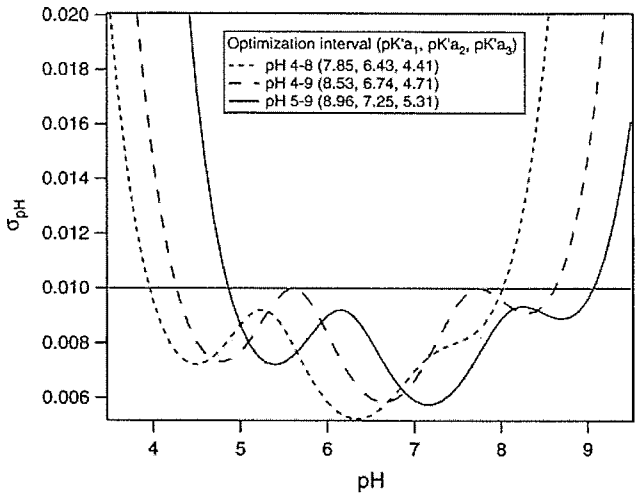

FIG. 7. Optimum pK'_{ai} values needed for an equal weight mixture of three dyes for various target pH intervals. Spectroscopic noise is assumed to be 0.001 OD units. Total dye concentration is 2×10^{-5} mol/kg. (Eq. 27: $p = 0.5$; $w_i = 1$).

fractions are kept unchanged, the standard deviations will uniformly increase by a factor of 1.5 across the pH range. The measurable pH range for the same standard deviation constraint of 0.01 units would be very much reduced (3.25 to 5.06 units and 6.58 to 8.49 units). However, if the dye mole fractions are optimized by accounting for the increased noise level, then the measurable pH range is much broader and covers 3.21 to 8.36 units. The importance of including the noise in the optimization process is also evident with further increase in the noise level to 0.002 OD units.

One can also choose dyes that will allow pH measurement over discontinuous pH intervals of interest. Thus with a two-dye mixture of, for example, phenol red ($pK'_{a1} = 7.79$) and bromophenol blue ($pK'_{a3} = 4.11$) where the pK'_{ai} values are separated by more than 3 pH units, one could target simultaneously the pH intervals on the low end (2.8–5.1 pH units) and the high end (6.6–8.7 pH units) with acceptable standard deviations of 0.01 pH units and without any sensitivity for the pH interval in between.

Other approaches have been reported to expand the pH range but they have their limitations. King and Kester[9] use forward modeling to generate three-dimensional plots of optical density as a function of wavelength and pH to pick optimum wavelengths. They then probe the sensitivity of the optical density ratio to pH to determine optimum concentrations. However, this type of forward modeling approach without optimization algorithms can become quite cumbersome in determining optimum mole fractions when, for example, there are more than two indicators in the mixture. Netto et al.[10] discuss the need to use indicators with similar color changes but do not discuss optimization with respect to mole fractions or pK'_{ai} values. Lin and Liu[11] use linearity of absorbance (optical density) at a chosen wavelength with respect to pH as the criteria for optimization. The use of absolute absorbance makes the measurement very susceptible to uncertainties in absolute dye concentration. The use of absorbance or optical density ratio, as we propose here, is more robust as it eliminates the dependence on dye concentration. Furthermore, the use of

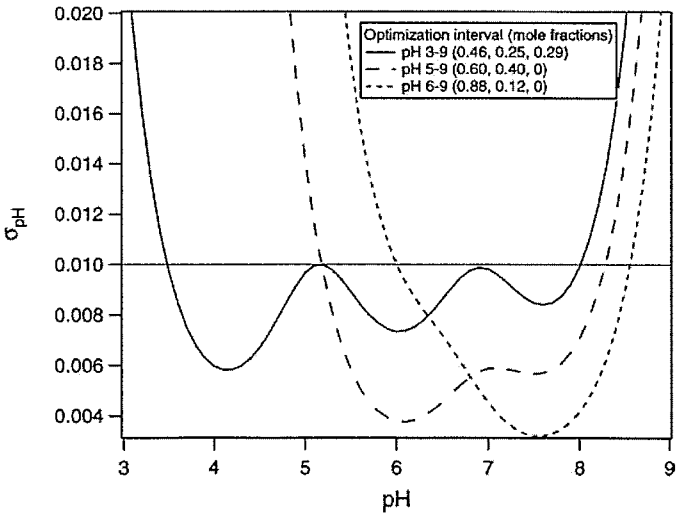

FIG. 6. Optimum dye mole fractions in the dye mixture change as the target pH interval changes. Spectroscopic noise is assumed to be 0.001 OD units. Total dye concentration is 2×10^{-5} mol/kg (Eq. 27: $p = 0.2$; $w_i = 1$).

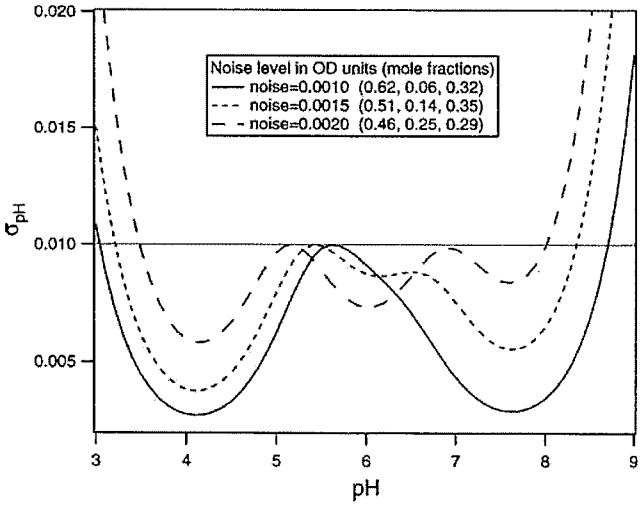

FIG. 8. Effect of noise in spectral measurement on optimization. Total dye concentration is 4×10^{-5} mol/kg (Eq. 27: $p = 0.2$; $w_i = 1$). Optimization interval for pH is 3 to 9 pH units.

absorbance ratio increases the sensitivity of the measurement as we take advantage of the fact that the optical density at the base wavelength increases with pH while the optical density at the acid wavelength simultaneously decreases with pH. The use of a linearity constraint for optimization, without consideration of the noise in the spectral data or precision needs of the measurement, could be quite severe as is seen by the need to use four indicators to cover a range of 4.5 pH units. Not only are we able to cover a similar range with three indicators, but also the standard deviation is lower. Note that the standard deviation as defined by Lin and Liu[11] refers to the deviation of the true spectral response from a linear model and is a systematic error arising out of model approximation. Random errors from experimental data will further increase this standard deviation. This is in contrast to our use of standard deviation that arises from noise in spectral data. Since we use the correct model spectral response, there is no additional systematic error contribution from this source.

It is important to note that none of the previous works account for the noise in spectral measurement and the role they play in the optimization process. This can be significant, as demonstrated in Fig. 8. The main advantages of our approach are that it uses an efficient formulation of the objective function that allows automated optimization for dye mole fractions and/or pK'_{ai} and also accounts for spectral noise. The output is in the form of a target pH range for a desired precision or the precision at each point over a desired pH range. Depending on the needs of the measurement and the desired precision and the optical noise in the system, one can determine the optimum dye formulation.

The method was tested in the laboratory using standard pH buffers. Phenol red, chlorophenol red, and bromophenol blue were calibrated to obtain their molar absorption coefficients and pK'_{ai} values using the standard techniques for single dyes outlined in the Introduction section (Table I). Note that phenol red can exist in a diprotic form at very low pH values.[5] Spectral measurements of phenol red at pH equal to 3, however, showed no interference from this diprotic form in the three-dye mixture that was formulated. Figure 9 shows the experimentally measured spectra in standard pH buffers ranging from 3 to 9. Note how the spectra show sensitivity over a wider pH range than was shown in Fig. 1 for a single dye. Figure 10a compares the model spectral response (Eq. 24) for the dye mixture using

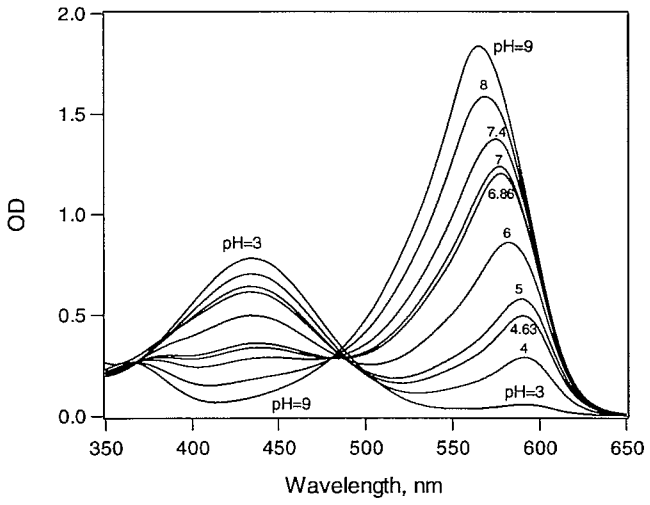

FIG. 9. Spectra of a three-dye mixture in standard buffer solutions with pH varying from 3 to 9 at 293 °K. Total dye concentration is 4×10^{-5} mol/kg. Spectral path length is 1 cm.

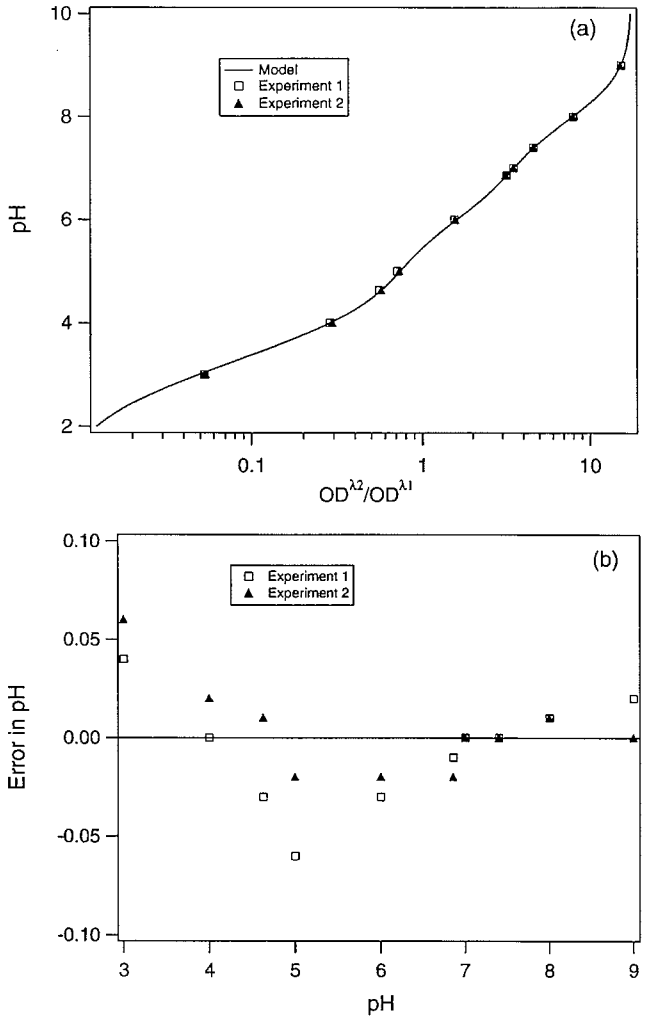

FIG. 10. (a) Comparing model and experimental data. The two wavelengths used are $\lambda_1 = 445$ and $\lambda_2 = 570$ nm. (b) Error in pH measurement is plotted as a function of pH. Total dye concentration is 4×10^{-5} mol/kg.

the dye parameters from Table I with two experimental data sets. Figure 10b plots the difference between the model-predicted pH and the true pH for these two data sets as a function of pH. Note that these errors include the fixed contributions arising out of any error in the calibration of pK'_{ai} values and molar extinction coefficients in addition to contribution from noise in spectroscopic measurements. The dye mixture is seen to work well over the range of buffers used from pH 3 to 9 and the advantage of using dye mixtures over single dyes that would be sensitive only over a range of 2 to 3 units is clearly seen.

We have recently developed calibration protocols for these dyes at high temperatures, pressures, and ionic strengths.[8] While these dyes retain their pH sensitivity and spectral features even after prolonged exposure to high temperatures, there is some thermal degradation that shows up as a reduced OD value. For single dyes, this is not an issue as the measurement is independent of dye concentration. Both the acid and base forms are reduced by the same factor and hence the ratio of their OD values is unaffected. For dye mixtures, however, this must be considered. Even though the measurement is independent of the volume of dye mixture added to the sample, it does depend on the individual dye mole fractions (Eq. 26). Thus, if the dyes in the mixture degrade by different amounts, the mole fractions are changed and this introduces an

error in calculation of pH if original mole fractions are used in the model. The degradation is a temperature–time effect with more degradation at higher temperatures and for longer time exposures. We have done a number of experiments in which the dye mixtures were exposed to high temperatures for various times. After this exposure, their performance was checked with spectral measurements using standard buffers at room temperature. For measurement errors of the same order as shown in Fig. 10b, the differential degradation, if any, was not considered to be an issue. At 323 °K, the dye mixture was observed to work well even after exposure for 12 months. At 373 °K, tests showed no measurable effect of heating for exposures up to 72 hours.

Such long-term temperature testing of dyes was critical to our first application of using these dye mixtures to make *in situ* high-temperature and high-pressure pH measurements of formation waters in oilfield wells. The use of a single reservoir of dye mixture to target a broad pH range is advantageous in dealing with space and weight constraints on oilfield logging tools. *In situ* pH measurements of formation waters in oil reservoirs have been made at temperatures ranging from 323 °K to 413 °K, pressures from 17 to 52 MPa, and ionic strength from 0.42 to 0.71 mol/kg.[7] Figure 11 shows real-time OD data from an appraisal well where a three-dye mixture was injected into a flowing formation water stream at 326.8 °K, 17 Mpa, and 0.71 mol/kg ionic strength. Details of the downhole sensor tool and the method for dye injection and data acquisition are reported in our earlier publication.[7] The OD values from the high-temperature, high-pressure spectrometer have been corrected for baseline using the OD values just prior to injection. The OD ratio at these two wavelengths has been used to calculate the pH using the models described in this paper. The mode of the dye injection causes slugs of varying dye concentrations to flow past the spectrometer (Cycles 1 through 7 in Fig. 11); however, as long as the total dye concentration is within the limits discussed in the Introduction section, pH calculation is not affected by the changing dye amounts. For oilfield waters, depending on their buffer strengths, acceptable dye concentrations are in the range of 2×10^{-5} to 8×10^{-5} mol/kg. The total concentration of the dyes in the second cycle is much higher than the upper limit so this section of the data is ignored. The dye concentrations in the fifth and sixth cycle are well within desired concentration limits, and the pH values for these cycles are determined by averaging the pH values over the 60–70 data points in each of those cycles. The fact that the pH does not change by more than 0.04 units across a range of higher dye concentrations in the other cycles indicates that this formation water is a strong buffer. The baseline is very steady and the good signal-to-noise ratio yielded standard deviations for Cycle 1 and Cycles 3 to 6 that were less than 0.005 pH units. In the seventh cycle, the total dye concentration is very low, resulting in a low signal-to-noise ratio and a higher scattering of data points in the pH trace. This cycle can also be ignored. Such simple, real-time quality checks result in a robust, high-quality measurement of the pH. This measurement was validated by collecting the formation water sample from this well for subsequent detailed water analysis in surface laboratories. Laboratory analysis at ambient conditions was used as input to simulate and model equilibria to downhole conditions of temperature and pressures in the oil well. The measured pH value of 6.26 units agreed very well with the predicted value of 6.29 units.[7]

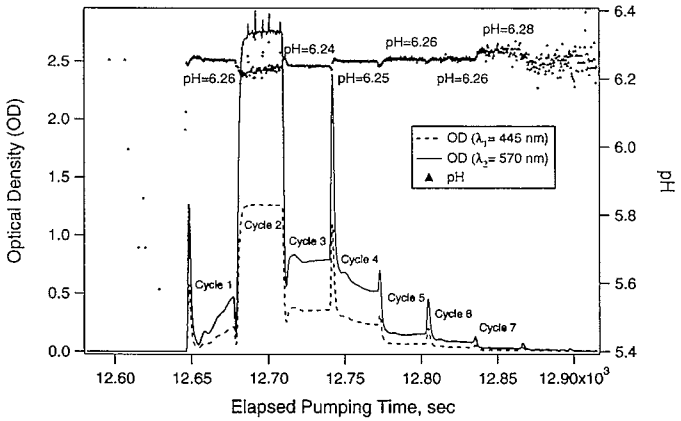

FIG. 11. Data acquired in real time from a downhole sensor developed for pH measurement of oilfield waters. The three-dye mixture was injected into a flowing water stream at 326.8 °K and 17.2 MPa. Spectral path length was 0.2 cm.

SUMMARY

An extended-range, high-accuracy spectroscopic pH measurement has been developed using mixtures of dyes. It has been demonstrated using a three-dye mixture on standard buffer solutions over a pH range of 3 to 9. It has also been successfully implemented for making real-time measurements of oilfield waters at high temperatures and pressures. Using optimized dye mixtures makes the spectroscopic pH measurement method more useful and removes a major limitation of the conventional single-dye spectroscopic method. The importance of proper selection of dyes has been demonstrated and algorithms developed to optimize dye formulations to achieve desired target accuracies for a pH measurement interval.

The pH measurement requires spectral data at a minimum of two wavelengths and is independent of amount of dye added to sample. It also requires only a one-time spectral calibration for the dyes to be used. The method is simple and easy to implement and is competitive with electrode methods that typically require frequent calibration and may be inaccurate at high temperatures, pressures, and ionic strengths due to liquid junction potential effects and reference electrode stability.

1. R. P. Buck, S. Rondini, A. K. Covington, F. G. K. Baucke, C. M. A. Brett, M. F. Camoes, M. J. T. Milton, T. Mussini, R. Naumann, K. W. Pratt, P. Spitzer, and G. S. Wilson, Pure Appl. Chem. **74,** 2169 (2002).
2. A. I. Vogel, *Text-Book of Quantitative Inorganic Analysis* (John Wiley and Sons, New York, 1961), 3rd ed.
3. R. Bates, *Determination of pH: Theory and Practice* (John Wiley and Sons, New York, 1964).
4. T. D. Clayton and R. H. Byrne, Deep-Sea Res. **40,** 2115 (1993).
5. W. Yao and R. H. Byrne, Environ. Sci. Technol. **35,** 1197 (2001).
6. T. D. Martz, J. J. Carr, C. R. French, and M. D. DeGrandpre, Anal. Chem. **75,** 1844 (2003).
7. B. Raghuraman, M. O'Keefe, K. O. Eriksen, L. A. Tau, O. Vikane, G. Gustavson, and K. Indo, SPE International Symposium on Oilfield Chemistry (Houston, Paper SPE 93057, February 2–4, 2005).
8. B. Raghuraman, G. Gustavson, O. Mullins, and P. Rabbito, AIChE J. **52,** 3257 (2006).
9. D. W. King and D. Kester, Appl. Spectrosc. **44,** 722 (1990).
10. E. J. Netto, J. I. Peterson, M. McShane, and V. Hampshire, Sens. Actuators B **29,** 157 (1995).
11. J. Lin and D. Liu, Anal. Chim. Acta **408,** 49 (2000).
12. P. R. Bevington and D. K. Robinson, *Data Reduction and Error Analysis for the Physical Sciences* (McGraw Hill, New York, 2003), 3rd ed., Chap. 3.
13. Visual Numerics Inc., IMSL Math Library: Fortran subroutines (1997).